# Interactions between conducting surfaces in salt solutions

Supplementary Information

October 2021

## 1 Normal pressure calculations

Here we derive expressions for the force across the midplane for our systems. In order to simplify the notation, we will derive expressions for the Canonical Ensemble. Extensions to the Grand Canonical Ensemble are straightforward. We want to calculate the free energy change when we vary the separation $h$ between the metallic electrodes to $h - \delta h$. This is obtained as

$$\beta \delta A = -\ln\left(\frac{Q(n, h-\delta h)}{Q(n,h)}\right) \tag{1}$$

where

$$Q(n,h) = \frac{1}{n!}\int_h dr_1 dr_2..dr_n e^{-\beta U(r_1, r_2..r_n, h)} \tag{2}$$

is the usual partition function for n charged particles between the electrodes separated by $h$ and with area S. Also $U(r_1, r_2..r_n, h)$ is the total electrostatic interaction, including image terms. (In the main paper, this energy was denoted $U_{C_0}$.) The subscript $h$ in the integral assumes the $z$ co-ordinate of each particle lies within the range $(0, h)$. That is, the electrodes are placed at $z = 0$ and $z = h$. We can write the ratio as follows,

$$\frac{Q(n, h-\delta h)}{Q(n,h)} = \frac{\int_h \prod_{k=1}^{n} \theta(z_k, \delta h) dr_1 dr_2..dr_n e^{-\beta U(r_1, r_2..r_n, h)}}{\int_h dr_1 dr_2..dr_n e^{-\beta U(r_1, r_2..r_n, h)}} \times \frac{\int_{(h-\delta h)} dr_1 dr_2..dr_n e^{-\beta U(r_1, r_2..r_n, h)}}{\int_h \prod_{k=1}^{n} \theta(z_k, \delta h) dr_1 dr_2..dr_n e^{-\beta U(r_1, r_2..r_n, h)}} \tag{3}$$

where

$$\theta(z, \delta h) = \begin{cases} 0, & \text{for } \frac{h}{2} < z < \frac{h}{2} + \delta h \\ 1, & \text{otherwise} \end{cases} \tag{4}$$

Now we note that we can write for the first factor on the RHS of eq. (3) (to $o(\delta h)$),

$$\begin{aligned} \frac{\int_h \prod_{k=1}^{n} \theta(z_k, \delta h) dr_1 dr_2..dr_n e^{-\beta U(r_1, r_2, .., r_n, h)}}{\int_h dr_1 dr_2..dr_n e^{-\beta U(r_1, r_2..r_n, h)}} \approx \\ 1 - \sum_{k=1}^{n} \frac{\int_h \theta(z_k, \delta h) dr_1 dr_2..dr_n e^{-\beta U(r_1, r_2..r_n, h)}}{\int_h dr_1 dr_2..dr_n e^{-\beta U(r_1, r_2..r_n, h)}} = 1 - n(\frac{h}{2})\delta h \end{aligned} \tag{5}$$

where $n(\frac{h}{2})$ is the density at the mid-plane. We now consider the denominator of the second factor on RHS of eq. (3),

$$\int_h \prod_{k=1}^{n} \theta(z_k, \delta h) dr_1 dr_2..dr_n e^{-\beta U(r_1, r_2..r_n, h)} = \int_{h-\delta h} dr_1 dr_2..dr_n e^{-\beta U(r_1', r_2'..r_n', h)} \tag{6}$$

where we have simply redefined the co-ordinates as follows:

$$r_i = (x_i, y_i, z_i) \text{ and } r_i' = \begin{cases} (x_i, y_i, z_i + \delta h), & \text{for } z_i > \frac{h}{2} \\ r_i, & \text{otherwise} \end{cases} \tag{7}$$

We rewrite this as,

$$\int_{h-\delta h} dr_1 dr_2..dr_n e^{-\beta U(r_1', r_2'..r_n', h)} = \int_{h-\delta h} dr_1 dr_2..dr_n e^{-\beta(U(r_1, r_2..r_n, h-\delta h)+\delta U)} \tag{8}$$

where

$$\delta U = U(r_1', r_2'..r_n', h) - U(r_1, r_2..r_n, h - \delta h) \tag{9}$$

Therefore,

$$\begin{aligned} \int_{h-\delta h} dr_1 dr_2..dr_n e^{-\beta(U(r_1, r_2..r_n, h-\delta h)+\delta U)} \approx \\ \int_{h-\delta h} dr_1 dr_2..dr_n e^{-\beta U(r_1, r_2..r_n, h-\delta h)}(1 - \beta \delta U) \end{aligned} \tag{10}$$

Dividing by the factor $\int_{h-\delta h} dr_1 dr_2..dr_n e^{-\beta U(r_1, r_2..r_n, h-\delta h)}$, we obtain the inverse of the second factor in eq.(3), $1 - \beta \langle \delta U \rangle_{h-\delta h}$, where $\langle ... \rangle_{h-\delta h}$ is the ensemble average in the $h - \delta h$ system. We thus arrive at:

$$\frac{Q(n, h - \delta h)}{Q(n, h)} = \frac{1 - n\frac{h}{2}\delta h}{1 - \beta \langle \delta U \rangle_{h-\delta h}} \tag{11}$$

Note that $\langle \delta U \rangle_{h-\delta h}$ is at least of order $\delta h$. Taking logarithms of both sides we obtain (to $o(\delta h)$),

$$\delta A = -\ln\left(\frac{Q(n, h - \delta h)}{Q(n, h)}\right) \approx n(\frac{h}{2})\delta h - \beta \langle \delta U \rangle_{h-\delta h} \tag{12}$$

We now rewrite the perturbation as

$$\delta U = U(1) + U(2) \tag{13}$$

where

$$\delta U(1) = U(r_1', r_2'..r_n', h) - U(r_1, r_2..r_n, h) \tag{14}$$

and

$$\delta U(2) = U(r_1, r_2..r_n, h) - U(r_1, r_2..r_n, h - \delta h) \tag{15}$$

We identify $-\frac{\delta U(1)}{\delta h} = F_{RHS}(ions)$ as the sum of forces on ions with $z > h/2$, which we abbreviate as RHS. Thus, the only non-zero force terms originate from ions and surface terms across the mid-plane. $-\frac{\delta U(2)}{\delta h} = F_{RHS}(surf)$ is the force on the right surface (at $z = h$), due to all ions. Substituting, and taking the limit of a vanishing $\delta h$, we have

$$-\beta \frac{\delta A}{\delta h} = n(\frac{h}{2}) + \beta \left\langle F_{RHS}(ions) \right\rangle_h + \beta \left\langle F_{RHS}(surf) \right\rangle_h \tag{16}$$

# 2 Ion density profiles

## 2.1 4 mM 3:1 salt, various separations

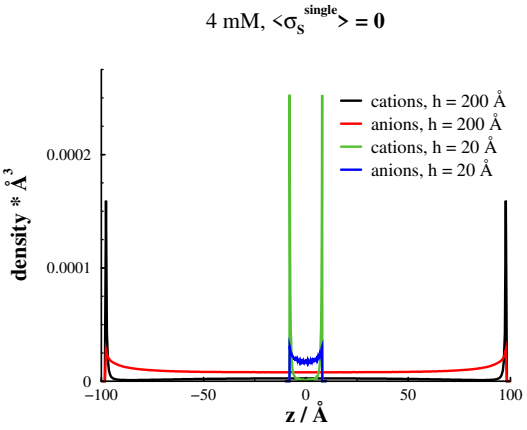


Figure 1: Ion density profiles, for the 4 mM 3:1 salt system, that displays net neutral surfaces (on average) at large separations.

We will initially focus on the 4 mM 3:1 salt system, with an applied potential adjusted so as to render the surfaces net neutral at large separations. Cat- and anion density profiles, at a large ($h = 200$ Å) and small ($h = 20$ Å) separation are shown, in Figure 1. Note that, even though the net contribution from the ideal pressure across the mid plane clearly is repulsive at $h = 20$ Å (since the total mid plane ion density is larger than in the bulk), strong ion correlation interactions across the mid plane render the overall net pressure to be attractive.

## 2.2 3:1 salt, $< \sigma_s^{single} > \approx -0.005\ e/\text{Å}^3$, various concentrations

In Figure 2, we compare scaled anion and cation density profiles, at various salt concentrations, with $< \sigma_s^{single} > \approx -0.005\ e/\text{Å}^3$. We recall from the main text (Figure 5) that these system display clear overcharging at 22 mM and 4 mM, and a very weak degree of overcharging at 1.4 mM, whereas the effective surfaces (outside the Stern layer) are "undercharged" at 0.23 mM. We can here see that the presence of overcharging, i.e. a local maximum of the apparent charge density outside the Stern layer, also can be (qualitatively) detected directly from the cation density profile. Specifically, this profile displays a local *minimum* outside the Stern layer if, and only if, overcharging takes place. This relation is present also for non-conducting surfaces, but a qualitative similarity, for conducting and non-conducting surfaces, is not there for the anions. With conducting surfaces, the anion density profiles display a local maximum, at all investigated salt concentrations, due to the attractive self-image interaction. Interestingly enough, when the salt concentration drops substantially below the overcharging threshold, the anion profile develops local *minimum*. We have, however not, ascertained if the occurrence of such a minimum perfectly coincides with the loss of overcharging.

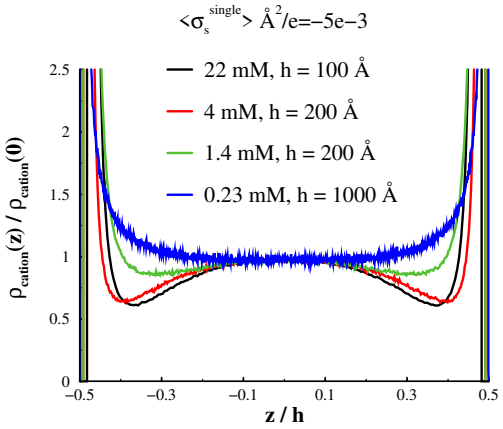


(a) Cation density profiles.

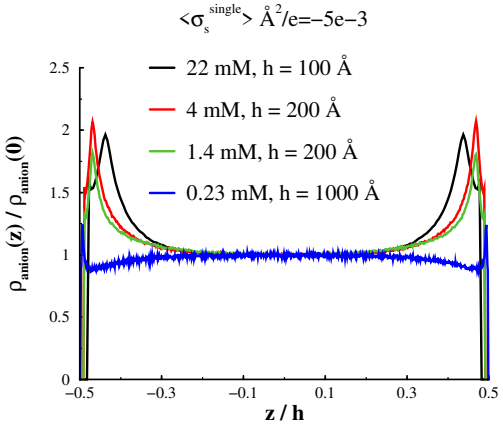


(b) Anion density profiles.

Figure 2: Density profiles of cations ($\rho_{cation}(z)$), and anions ($\rho_{anion}(z)$) for 3:1 salt solutions at various concentrations, with the applied potential adjusted such that $< \sigma_s^{single} > \approx -0.005\ e/\text{Å}^3$. In order to facilitate comparisons, the $z$ values are scaled by the separations at which the simulations were performed, and the ion densities are scaled by their respective mid plane value.